Distinct functions of receptor-like tyrosine phosphatases CD45 and CD148 in chemoattractant-mediated neutrophil migration and response to S. *aureus* infection

Jing W. Zhu[1], **Kristin Doan**[1], **Jason Park**[2,5], **Angela H. Chau**[2,5], **Hong Zhang**[3], **Clifford A. Lowell**[4], and **Arthur Weiss**[1,*]

[1]Departments of Medicine and of Microbiology and Immunology, Howard Hughes Medical Institute, Rosalind Russell Medical Research Center for Arthritis, University of California, San Francisco, San Francisco, CA, 94143-0795, USA

[2]Department of Cellular and Molecular Pharmacology, University of California San Francisco, California 94158, USA

[3]Department of Research and Development, BioLegend INC, 11080 Roselle Street, San Diego, CA 92121

[4]Department of Laboratory Medicine University of California, San Francisco, San Francisco, CA, 94143, USA

[5]UCSF/UC Berkeley Joint Graduate Group in Bioengineering

Abstract

Neutrophils, critical innate immune effectors, use bacterial-derived chemoattractant-induced G-protein coupled receptor (GPCR) signaling for their pursuit of bacteria. Tyrosine phosphorylation pathways and receptor-like tyrosine phosphatases (RPTPs) are rarely considered in chemoattractant-mediated GPCR signaling. Here, we report that two RPTPs CD45 and CD148, previously shown to share redundant roles in positively regulating Src Family Kinases (SFKs) in immunoreceptor signaling pathways in B cells and macrophages, are critical in the neutrophil response to *S. aureus* infection and, surprisingly, in chemoattractant-mediated chemotaxis. Remarkably, deficiency in either of these RPTPs influenced neutrophil GPCR responses in unique ways. Our results reveal that CD45 positively while CD148 positively and negatively regulate GPCR function and proximal signals including Ca^{2+}, phosphatidylinositol 3′OH kinase (PI(3)K) and phosopho-extracellular regulated kinase (pERK) activity. Moreover, our results suggest that CD45 and CD148 preferentially target different SFK members Hck and Fgr vs Lyn, respectively, to positively and negatively regulate GPCR pathways.

Introduction

Neutrophil migration toward bacterial chemoattractants is critical for anti-bacterial responses (Viola and Luster, 2008). Bacterial-derived chemoattractants such as formyl-Met-Leu-Phe (fMLF) can induce directed-cell migration (also called chemotaxis) via the

---

*Correspondence: aweiss@medicine.ucsf.edu.

activation of G-protein coupled receptors (GPCRs) (Murphy, 1994). Chemoattractant receptors couple to the heterotrimeric guanine nucleotide-binding protein Gi to transduce intracellular signals. After fMLF binds to its GPCR, the Gα and Gβγ subunits of Gi dissociate. The Gβγ subunits are thought to activate the β isoforms of phospho-lipase C (PLC) (Wu et al., 1993) with the consequent mobilization of intracellular calcium stores, and diacyglycerol The Gβγ subunits also activate phosphatidylinositol-3-OH kinase (PI3K) gamma, leading to increases in membrane phosphatidylinositol-3,4,5-triphosphate (PIP_3) (Stephens et al., 1994; Stoyanov et al., 1995). PI3K deficient neutrophils exhibit severe defects in migration and respiratory burst in response to chemotactic agents, suggesting that generation of PIP_3 is important for fMLF-induced chemotaxis (Sasaki et al., 2000). It has been reported that tyrosine kinase pathways are activated by the GTP-bound G protein subunits (Luttrell et al., 1999).

Src family kinases (SFKs) are implicated in GPCR signaling pathways. Lyn, Hck and Fgr are the three SFKs that are predominantly expressed in neutrophils. Studies using $Hck^{-/-}Fgr^{-/-}Lyn^{-/-}$ neutrophils and treatment with the SFK inhibitor PP2 identify a role for SFKs in fMLF-induced degranulation responses (Mocsai et al., 2000; Mocsai et al., 1999). Hck and Fgr appear to be required for an fMLF-triggered neutrophil respiratory burst and F-actin polymerization (Fumagalli et al., 2007). In contrast to the Hck and Fgr SFKs, Lyn is unique since it has both positive and negative roles in a variety of receptor-mediated signaling pathways. Disruption of the *Lyn* gene in mice results in the development of myeloproliferation and autoimmunity (Chan et al., 1997; DeFranco et al., 1998; Hibbs et al., 1995; Nishizumi et al., 1995; Yu et al., 2001). These results reveal predominantly negative roles for Lyn *in vivo.* However, despite intensive studies on their roles in growth factor and antigen receptor pathways, far less is known about how and where SFKs fit into the classical GPCR signaling pathways.

Within hematopoietic cells, the clearest function of SFKs has been defined in immunoreceptor signaling, where the receptor contains two common immunoreceptor tyrosine-based activation motifs (ITAM). By phosphorylating the two tyrosines in he ITAMs, SFKs invariably initiate signaling, leading to the recruitment of the tandem-SH2 domains of Syk kinases. In integrin and chemokine receptors, even though it has been shown that SFKs are required, their functions are also less completely understood.

Given their central roles in receptor signaling and immune cell function, the regulation of SFKs has been intensively investigated (Hermiston et al., 2002; Hermiston et al., 2009). SFKs have two regulatory tyrosine phosphorylation sites (Bjorge et al., 2000). Trans-autophosphorylation of the kinase activation loop tyrosine leads to an increase in catalytic activity. Phosphorylation of a tyrosine in the SFK C-terminal tail by the C-terminal Src kinase (Csk) leads to stabilization of an autoinhibited closed conformation (Sicheri and Kuriyan, 1997). Just as kinases regulate the phosphorylation of these sites, their dephosphorylation is also regulated.

The receptor-like protein tyrosine phosphatase (RPTP) CD45 (encoded by *Ptprc*) dephosphorylates the inhibitory tyrosine of the SFKs in most hematopoietic cells, as best defined in T cells as the CD45 deficient mice showed a profound T cell developmental block (Hermiston et al., 2003) (Byth et al., 1996; Kishihara et al., 1993; Mee et al., 1999). Although CD45-deficiency has a B cell phenotype, it is much milder than in T cells. The reason for the discordancy in the two lineages is expression of another RPTP, CD148 (encoded by *Ptprj*). CD148 functions redundantly with CD45 to regulate SFK activity in B cells and macrophages in ITAM-immunoreceptor stimulation (Zhu et al., 2008). Compared to CD45, relatively less is known about the function of CD148. In contrast to the tandem PTP domains of CD45, CD148 has only a single PTP homology domain. Whereas CD45 is

expressed exclusively in hematopoietic cells, CD148 is expressed in and outside the hematopoietic lineage (Gaya et al., 1999; Lin et al., 2004). The purpose of coexpression of CD45 and CD148 on many hematopoietic cell lineages is not clear, but one intriguing possibility is to regulate distinct substrates or distinct signaling pathways. Based on the redundant role of CD45 and CD148 in immunoreceptor signaling and their overlapping expression on most hematopoietic cells (Zhu et al., 2008), we wondered whether CD45 and CD148 might regulate other non-ITAM mediated signaling pathways such as GPCR-mediated responses.

The co-expression of CD45 and CD148 in immune cells has likely been selected to maximize host defense to microbial infection. Here, we have investigated potential functions of CD45 and CD148 in neutrophil-responses to bacteria. Our data reveal a critical role for either CD148 or CD45 during the host response to *Staphylococcus aureus* (*S. aureus*). Additionally, we found unexpectedly distinct functions for CD45 and CD148 in regulating chemoattractant-induced migration of neutrophils during infection. Our biochemical studies suggest that CD45 and CD148 regulate this GPCR pathway in unique ways, where they function upstream of calcium, MAP kinase and PI3K pathways, by preferentially targeting different SFK members.

Results

CD45 and CD148 both function in the clearance of bacteria

We previously reported that $Ptprc^{-/-}$ and $Ptprj^{TM-/TM-}$ (functional inactivation via deletion of the exon encoding the CD148 transmembrane domain) doubly deficient mice die prematurely (Zhu et al., 2008). However, antibiotic treatment delayed the death of a substantial number of $Ptprc^{-/-}Ptpri^{TM-/TM-}$ doubly deficient mice (Fig. 1A). This result supports the notion that disruption of these two phosphatases perturbs host defense, likely including bacterial resistance. To assess the role of CD45 and CD148 in mediating bacterial clearance in a simple model system that allows for quantitative assessment of bacteria burden and a localized neutrophil response, mice were infected with *S. aureus* in an air pouch that was experimentally generated on the back of the torso. Clearance of *S. aureus* in the air pouch model is largely dependent on neutrophils (Kim et al., 2008; Li et al., 2002), which make up >90% of the recruited cells. Although $Ptprc^{-/-}$ mice were unable to clear the bacteria as successfully as wild type mice, $Ptprj^{TM-/TM-}$ mice were more efficient than either when assessed 24 hours post-infection (Fig. 1B). Interestingly, $Ptprc^{-/-}Ptpri^{TM-/TM-}$ mice had a more severe defect than $Ptprc^{-/-}$ mice in clearing the bacteria, suggesting that CD148 contributed both a positive and a negative regulatory role to this process. This result was intriguing since this was the first time $Ptprc^{-/-}$ and $Ptprj^{TM-/TM-}$ mice showed distinct rather than merely redundant effects *in vivo*. We also assessed the recruitment of neutrophils to the site of this localized infection. At 24 hours post-infection, despite the significantly different numbers of bacteria in the air pouches (Fig. 1B), the number of neutrophils recruited was similar in each of the different mouse strains (Fig. 1C). Since greater numbers of *S. aureus* would naturally provide a stronger chemoattractant signal for neutrophil migration through elaboration of bacterial derived factors such as formylated peptides, we sought to fix the number of organisms in the pouch by injection of heat-killed *S. aureus* and examine an earlier time point. At 6 hours following injection of heat-killed bacteria, $Ptprc^{-/-}$ mice contained reduced numbers of neutrophils recruited to the air pouch, whereas $Ptprj^{TM-/TM-}$ mice showed significantly greater neutrophil recruitment, compared to wild-type animals (Fig. 1D). Neutrophil recruitment in $Ptprc^{-/-}Ptpri^{TM-/TM-}$ mice was equivalent to wild-type, perhaps reflecting the complex and opposite effects of the roles of both RPTPs examined at a single time point. Nonetheless, these results suggested that differential recruitment of neutrophils to the infected air pouch may contribute to the differences in bacterial clearance between CD45 and CD148 deficient mice.

Redundant regulation of neutrophil adhesion, phagocytosis, superoxide production and bacterial killing by CD45 and CD148

Bacterial clearance by neutrophils *in vivo* is a complex process involving chemotaxis, cell adhesion, phagocytosis, superoxide release, bacterial killing and other processes. Although the distinct numbers of neutrophils in the airpouch after 6 hours suggested the possibility of unique influences of the RPTPs on chemotaxis, we sought to broadly explore explanations for the different abilities of neutrophils in $Ptprc^{-/-}$ and $Ptprj^{TM-/TM-}$ mice to mediate bacterial clearance.

The importance of cell adhesion for stimulation of phagocyte function has been well recognized. It has been demonstrated that, for neutrophils, an activating signal from adhesion requires β2 integrins (Jakus et al., 2007). We first examined integrin-mediated cell adhesion using purified bone marrow neutrophils. $Ptprc^{-/-}$, $Ptprj^{TM-/TM-}$ as well as $Ptprc^{-/-}Ptpri^{TM-/TM-}$ neutrophils were all equally impaired to a partial extent in integrin (RGD-peptide)-induced cell adhesion (Fig 2A). Cell adhesion that was induced by the bacteria-derived chemoattractant fMLF (*N*- formyl-methionyl-leucyl-phenylalanine) produced similar results (data not shown). These results indicate that CD45 and CD148 partially regulate cell adhesion, but do so redundantly.

SFKs have been implicated in the events controlling Fc receptor mediated phagocytosis (Fitzer-Attas et al., 2000). Therefore, we examined the phagocytosis of complement-opsonized bacteria by flow cytometry. Whereas the $Ptprc^{-/-}$ or $Ptprj^{TM-/TM-}$ neutrophils each displayed comparable subtle reductions in *S. aureus* phagocytosis, $Ptprc^{-/-}Ptpri^{TM-/TM-}$ neutrophils were more impaired, with a greater than 50% reduction in the phagocytosis compared to wild-type neutrophils (Fig. 2B).

The requirement for neutrophil superoxide production in host defense against *S. aureus* has been well documented both in human patients with chronic granulomatous disease (Liese et al., 2000) and in mouse mutants lacking subunits of nicotinamide adenine dinucleotide phosphate (NADPH) -oxidase (Ellson et al., 2006; Pollock et al., 1995). After stimulation, neutrophils from either of the individually deficient $Ptprc^{-/-}$ or $Ptprj^{TM-/TM-}$ mice produced less superoxide than wild-type neutrophils *in vitro*. However, the defect in superoxide production from $Ptprc^{-/-}Ptpri^{TM-/TM-}$ neutrophils was much more severe than either single mutant (Fig. 2C). We next assessed the ability of neutrophils to kill internalized bacteria. In this assay, only the $Ptprc^{-/-}Ptpri^{TM-/TM-}$ neutrophils exhibited reduced ability to kill internalized *S. aureus* (Fig. 2D). Thus, these results demonstrate that CD45 and CD148 play redundant functions in regulating neutrophil adhesion, phagocytosis, superoxide release and bacterial killing.

These findings on cell adhesion, phagocytosis, superoxide generation and bacterial killing suggest that these neutrophil functions do not likely account for the increased ability of CD148 deficient mice to mediate better bacterial clearance of *S. aureus* in the air pouch model depicted in Figure 1B. However, the loss of both of these RPTPs clearly reduces neutrophil function to the point that the $Ptprc^{-/-}Ptpri^{TM-/TM-}$ mice are unable to clear *S. aureus* infection in the air pouch model.

CD45 and CD148 regulate neutrophil chemotaxis in a distinct ways

When in the proximity of infection, neutrophils detect end-target chemoattractants, such as bacterial fMLF that helps them migrate towards the infection site (Foxman et al., 1997; Heit et al., 2002). In order to study this pathway, we used fMLF as a simplified model bacterial chemoattractant. To examine the migratory response in more detail, purified neutrophils were exposed to a gradient of fMLF in EZ-TAXIScan chambers. In response to the chemoattractant, wild type neutrophils migrated towards the gradient of fMLF (Fig. 3A and

suppl. movies M1-4). Disruption of *Ptprc* and loss of CD45 resulted in a marked impairment of chemotaxis; cells migrated over a much shorter distance with slower speed. Quite strikingly, and in contrast, more $Ptprj^{TM-/TM-}$ cells migrated farther, faster and more directionally up the gradient of fMLF than even the wild type cells did (Fig. 3B). It was also noteworthy that a greater proportion of $Ptprj^{TM-/TM-}$ neutrophils were in a highly migratory state compared to wild type cells (suppl. Fig. 1 and suppl. movies M1-3). $Ptprc^{-/-}Ptpri^{TM-/TM-}$ neutrophils showed very little response to fMLF (Fig. 3A, B, suppl. Fig. 1 and suppl. Movies M4).

With all the assays assessed so far, we noticed a good correlation of the $Ptprc^{-/-}$ functional impairment in bacterial clearance with assays of cell adhesion, phagocytosis, superoxide release, as well as chemotaxis. In sharp contrast, despite of partial impairment in cell adhesion, phagocytosis, and superoxide release, $Ptprj^{TM-/TM-}$ mice cleared the bacteria better than wild type. This paradoxical *in vivo* result correlated best with the increased neutrophil recruitment and chemotaxis observed with $Ptprj^{TM-/TM-}$ mice. These findings suggest that the distinct functional abilities of CD45 and CD148 neutrophils in regulating GPCR-mediated chemotactic responses could account for the difference in bacterial clearance *in vivo*.

CD45 and CD148 differentially regulate signaling events in chemotaxis

We demonstrated the opposite effects of CD45 and CD148 expression on neutrophil chemotaxis where they are co-expressed. Surprisingly, these opposite effects were observed in a GPCR signaling system, which is not normally associated with protein tyrosine phosphorylation pathways. Therefore, we focused on understanding the molecular mechanisms underlying the differences between CD45 and CD148 in regulating chemoattractant-guided migration. We first examined chemoattractant-receptor induced intracellular free calcium concentration ($[Ca^{2+}]_i$) changes. To eliminate possible integrin effects, neutrophil responses were assessed in suspended, rather than adherent, cells. At a high dose of fMLF, comparable increases in $[Ca^{2+}]_i$ in neutrophils from all 4 genotypes were observed (Fig. 4A). However, at lower doses of fMLF, we observed opposite effects of CD45 or CD148 deficiency upon $[Ca^{2+}]_i$ increases (Fig. 4B and 4C). Interestingly, $Ptprj^{TM-/TM-}$ neutrophils were hyperresponsive to fMLF stimulation, whereas $Ptprc^{-/-}$ neutrophils exhibited an impaired response. $Ptprc^{-/-}Ptpri^{TM-/TM-}$ neutrophils showed an even more severe impairment. Equal elevations of $[Ca^{2+}]_i$ following ionomycin (Fig. 4D) or thapsigargin (data not shown) addition to neutrophils of all genotypes, indicated that the differences in responses to low doses of fMLF were not due to defects in intracellular calcium stores or in capacitative calcium entry.

The phosphatidylinositol-3-OH kinase (PI3K) pathway acts downstream of GPCRs in many chemotaxis models (Liu et al., 2007; Sasaki and Firtel, 2006; Sasaki et al., 2000; Stephens et al., 2002). Therefore, we examined the importance of CD45 and CD148 in regulating Akt, a downstream effector of the PI3K pathway following fMLF stimulation, using a phospho-flow based assay. Similar to the $[Ca^{2+}]_i$ responses, a greater increase in phosphorylation of Akt was observed in $Ptprj^{TM-/TM-}$ neutrophils compared to wild-type type cells (Fig. 5A). In contrast, impaired induction of Akt phosphorylation was detected in $Ptprc^{-/-}$ neutrophils, and inducible Akt phosphorylation was almost completely eliminated in $Ptprc^{-/-}Ptpri^{TM-/TM-}$ cells. Very similar trends in responses were also observed for fMLF induction of extracellular regulated kinase (ERK) 1 and 2 phosphorylation, as determined by flow cytometry (Fig 5B).

Disruption of SFK function impairs fMLF induced GPCR signaling

Our previous studies demonstrated that, in B cells and macrophages, CD45 and CD148 function redundantly to dephosphorylate the inhibitory tyrosine residue on SFKs, thereby positively regulating immunoreceptor-ITAM regulated pathways (Zhu et al., 2008). Therefore, the effects of the deficiency of these RPTPs might phenocopy deficiencies in SFKs. To compare the phenotype of CD45 and CD148 doubly-deficient neutrophils with the phenotype of cells derived from SFK deficient mice, we examined $[Ca^{2+}]_i$ changes following-fMLP stimulation in $Hck^{-/-}Fgr^{-/-}Lyn^{-/-}$ deficient neutrophils. Hck, Fgr and Lyn kinases are the main SFK present in neutrophils and, by analogy to B cells, macrophages and platelets, represent likely substrates for CD45 and CD148. Like $Ptprc^{-/-}$ and $Ptprc^{-/-}Ptprj^{TM-/TM-}$ neutrophils, $Hck^{-/-}Fgr^{-/-}Lyn^{-/-}$ neutrophils showed a impaired $[Ca^{2+}]_i$ increase in response to fMLF stimulation (Fig. 6A). Treatment of wild-type neutrophils with the SFK inhibitor PP2 to acutely inhibit catalytic function of all three SFKs resulted in a similar impairment of intracellular free calcium increase, suggesting the defect we observed in $Hck^{-/-}Fgr^{-/-}Lyn^{-/-}$ mice was not due to altered neutrophil development in the absence of SFKs (Fig. 6B). These results support the notion that SFKs play an important role in the GPCR-coupled fMLF receptor signaling responses.

In light of the discrepancy between the phenotype of $Hck^{-/-}Fgr^{-/-}Lyn^{-/-}$ and $Ptprj^{TM-/TM-}$ neutrophils, we hypothesized that CD45 and CD148 preferentially target distinct SFKs in the GPCR pathway. Accumulating reports suggest that Lyn establishes signaling thresholds by acting as both a positive as well as a negative modulator of a variety of signaling responses (Chan et al., 1997; DeFranco et al., 1998; Hibbs et al., 2002; Hibbs et al., 1995; Nishizumi et al., 1995). Furthermore, Lyn has been implicated as a negative regulator of fMLF responses in neutrophils (H Zhang and C Lowell unpublished data). Therefore, we hypothesized that CD148 preferentially regulates Lyn, the SFK member which is characterized to play a negative regulatory role. In contrast, we propose that CD45 predominantly positively regulates Hck and Fgr, or is simply less selective in regulating SFK, thereby positively regulating the GPCR pathway (suppl. Fig. 4). To test this hypothesis, we first examined changes in $[Ca^{2+}]_i$ following fMLF stimulation in single $Lyn^{-/-}$ or doubly-deficient $Hck^{-/-}Fgr^{-/-}$ neutrophils. Indeed, like the $Ptprj^{TM-/TM-}$ cells, Lyn-deficient neutrophils manifested elevated $[Ca^{2+}]_i$ responses to fMLF stimulation (Fig. 6C). In contrast, $Hck^{-/-}Fgr^{-/-}$ neutrophils showed a slight decrease in $[Ca^{2+}]_i$ responses to fMLF stimulation compared to wild-type (Fig. 6D), which contrasted with the impairment seen in the $Hck^{-/-}Fgr^{-/-}Lyn^{-/-}$ mice, presumably because of some residual positive regulatory function provided by Lyn. To further compare the phenotypes of RPTP-deficient with SFK-deficient neutrophils, we examined fMLF induced ERK1 and 2 phosphorylation in $Lyn^{-/-}$ and $Hck^{-/-}Fgr^{-/-}$ cells. Consistent with the $[Ca^{2+}]_i$ responses, $Lyn^{-/-}$ neutrophils showed elevated induction of ErK1 and 2 activity, whereas the responses of $Hck^{-/-}Fgr^{-/-}$ neutrophils were similar to those of wild-type cells (Fig. 6E).

We next examined chemotaxis with SFK-deficient neutrophils using the EZ-TAXIScan, as before. Similar to what we observed in $Ptprj^{TM-/TM-}$ neutrophils, more $Lyn^{-/-}$ neutrophils migrated toward the gradient of fMLF, and those cells that migrated had longer tracks over a fixed time period than wild type cells (Fig. 6F and suppl. movies M5-6). In contrast, $Hck^{-/-}Fgr^{-/-}$ cells migrated similarly to wild type cells toward fMLF (suppl. Fig. 3 and data not shown). These studies indicate that either CD148- or Lyn kinase-deficiency results in increasing chemotactic activity in response to chemoattractant fMLF. This is likewise associated with increased signaling by the fMLF-stimulated GPCR, as evidenced by increased $[Ca^{2+}]_i$ elevations and increased phospho-ERK. Collectively, the observations suggest that CD148 preferentially regulates Lyn (suppl. Fig. 4). In contrast, CD45-deficient cells mimic the SFK-deficient neutrophils, suggesting that this phosphatase is less selective in regulating SFKs.

CD45 and CD148 have distinct selectivities toward different SFKs

The functional correlates between the responses of neutrophils from CD45 or CD148 and SFKs deficient mice further supports our hypothesis regarding distinct selectivities of CD45 and CD148 toward different SFKs. To directly test this hypothesis biochemically, we studied the phosphorylation status of the C-terminal inhibitory tyrosine residue of different SFKs. We used monoclonal antibodies that are specific for Lyn or Hck to immunoprecipitate individual SFK from neutrophils and then detected the phosphorylation status of the inhibitory tyrosine at their C-termini (Fig. 7A). The specificities of the antibodies were confirmed using cell lysates from $Lyn^{-/-}$ or $Hck^{-/-}$ neutrophils as controls (Fig. 7A). Compared to wild type cells, $Ptprc^{-/-}$ neutrophils showed elevated phosphorylation of the inhibitory tyrosine residue of Hck. No obvious difference on phosphorylation was observed in $Ptprj^{TM-/TM-}$ from wild type. Importantly, the comparative amount of the phosphorylation of the inhibitory tyrosine on Hck was similar in $Ptprc^{-/-}$ and $Ptprc^{-/-}$ $Ptprj^{TM-/TM-}$ cells (Fig. 7A), suggesting that CD45, but not CD148, dephosphorylates this tyrosine residue. Although we were unable to detect a change in phosphorylation of the C-terminal inhibitory tyrosine of Lyn in $Ptprj^{TM-/TM-}$, we consistently observed that the amount of Lyn was decreased in $Ptprj^{TM-/TM-}$ cells. Moreover, and in contrast to Hck, the inhibitory tyrosine of Lyn was phosphorylated to a greater extent in $Ptprc^{-/-}$ $Ptprj^{TM-/TM-}$ cells than in $Ptprc^{-/-}$ cells (Fig. 7A). Together, these observations indicate the C-terminal inhibitory tyrosine of Lyn is regulated by both CD45 and CD148. Note, the phosphorylation status of inhibitory tyrosine did not substantially change following fMLF stimulation (data not shown), suggesting CD45 and CD148 regulate SFKs predominantly at the basal state in neutrophils.

In many systems, Lyn exerts its negative regulatory role by phosphorylating immunoreceptor tyrosine-based inhibitory motifs (ITIMs), thereby recruiting inhibitory phosphatases, such as Src homology 2 (SH2) domain containing protein tyrosine phosphatase (SHP)-1 (suppl. Fig. 4) (Lowell, 2004). We tested this hypothesis by assessing the phosphorylation status of SHP-1 in mutant neutrophils following fMLF stimulation. The tyrosine phosphorylation of SHP-1 positively correlates with its activity (Zhang et al., 2003). Strikingly, in the basal state, $Ptprc^{-/-}$ neutrophils showed markedly elevated SHP-1 phosphorylation. No substantial difference in SHP-1 phosphorylation was noted between unstimulated wild-type and $Ptprj^{TM-/TM-}$ neutrophils. Following fMLF stimulation, we consistently observed an early transient reduction of SHP-1 phosphorylation in wild-type and $Ptprc^{-/-}$ neutrophils followed by increased phosphorylation at later time points, suggestive of a negative feedback circuit. In contrast, the phosphorylation of SHP-1 in $Ptprj^{TM-/TM-}$ neutrophils consistently remained low even at longer time points (Fig. 7B). These results are consistent with our hypothesis that CD148 predominantly regulates an inhibitory pathway through Lyn that can lead to SHP-1 phosphorylation and activation (presumably via phosphorylation and recruitment to an ITIM-containing receptor), while CD45 with less preference, targets Lyn, Hck and Fgr, thereby positively regulating chemoattractant signaling (suppl. Fig. 4).

Discussion

The function of RPTPs in chemoattractant-mediated GPCR signaling has not previously been appreciated. In this study, we found that the two RPTPs CD45 and CD148 have critical and unique as well as redundant functions in a chemoattractant-GPCR signaling pathway. Our studies along these lines were initiated by the unexpected finding that the loss of CD45 or CD148 has distinct and opposite influences on neutrophil-dependent bacterial clearance in the skin air pouch model. We sought a mechanistic explanation for these discordant effects. The observed redundant deficits in neutrophil functions, such as in cell adhesion, phagocytosis, respiratory burst and bactericidal activity are in line with our previous

observations of the redundant influence of these RPTPs in ITAM-coupled receptor signaling systems in macrophages and B cells (Zhu et al., 2008). The functional impairments of neutrophils from $Ptprc^{-/-}$ mice likely contribute to their relatively weaker host defense. However, the early increased neutrophil recruitment as well as the increased chemotatic responses and fMLF receptor signaling of neutrophils from $Ptprj^{TM-/TM-}$ mice was surprising, but correlated with their ability to more rapidly clear the infection. This increased responsiveness by CD148 deficient cells is unique and in marked contrast to the reduced responsiveness of $Ptprc^{-/-}$ neutrophils. However, these RPTPs do have some overlap in their functional activities, as revealed in the $Ptprc^{-/-}Ptpri^{TM-/TM-}$ mice. Deficiency of both of these RPTPs much more substantialy impaired overall neutrophil function. These redundant functions in regulating SFKs likely accounts for the more profound impairment in resistance to *S. aureus* infection in the $Ptprc^{-/-}Ptpri^{TM-/TM-}$ animals and the more profound defects observed in most of the signaling and functional assays.

The role of RPTPs in *S. aureus* infection is complex. In this paper we chose to focus on a localized infection model, the air pouch, and to understand the unexpected non-redundant function of CD45 versus CD148 in the fMLF signaling pathway. Previously, we found that these RPTPs have only redundant functions in ITAM receptor-mediated signaling pathways in B cells and macrophages (Zhu et al., 2008). Directly correlated with the differential host defense and migratory responses of CD45 versus CD148 deficient neutrophils is the differential effect of these RPTPs on GPCR-mediated signaling responses. CD148-deficient cells consistently demonstrated increased signaling responses (Ca^{2+} flux, Erk and Akt phosphorylation) while CD45-deficient cells were modestly impaired compared to wild-type cells. This differential effect on intracellular signaling mirrors some of the differences that have been genetically revealed in studies of the main substrates of these RPTPs; namely the SFKs. In our experiments, neutrophils from Lyn kinase-deficient mice manifested the same increased fMLF signaling response as cells from CD148-deficient animals. Loss of all three SFKs produced a signaling defect closely resembling $Ptprc^{-/-}Ptpri^{TM-/TM-}$ cells. These observations suggest that at least in the GPCR pathway the preferential regulation, presumably involving dephosphorylation, of Lyn by CD148 versus CD45, accounts for the unexpected non-redundant functions for these RPTPs.

The differential function of Hck and Fgr versus Lyn kinase in GPCR pathways has been incompletely studied. Clearly, all three kinases are involved responses to end-target chemoattractants, such as fMLF, as we have shown here. Surprisingly, Hck and Fgr have the opposite function in GPCR pathways stimulated by endogenous chemokines such as MIP-1α (CCL3) and MIP2 (CXCL2) (Zhang et al., 2005). Neutrophils lacking Hck and Fgr show increased responses to these chemokines while Lyn-deficient cells shown only a modest impairment in response to these stimuli (H. Zong and C. Lowell, unpublished). However, the signaling pathways downstream of distinct receptors involved in chemotaxis seem to differ. For instance, it has been reported that end-target chemoattractants (such as fMLF) and endogenous chemokines (such as IL-8, MIP-2) induce different signaling pathways; end-target attractants require PI3K, whereas endogenous chemokines signal independently of PI3K but activate p38 mitogen activated protein kinases (Heit et al., 2002). We have also tested the consequences of the loss of CD45 and CD148 in neutrophils following stimulation with MIP-2, an endogenous chemokine. In preliminary studies, we found that their effect on intracellular calcium following MIP-2 were quite different than during fMLF stimulation (supp. Fig.2), with essentially an opposite pattern of responses observed. This suggests that CD45 and CD148 may regulate exogenous- and endogenous-chemokine mediated signaling pathways in essentially opposite ways, similar to Hck and Fgr versus Lyn kinases. This further supports the notion that CD148 is primarily responsible for Lyn activation while CD45 has broader, but incomplete activity, on all three SFK.

The discovery of unique functions of CD45 and CD148 following GPCR stimulation extended our knowledge beyond their redundant roles in Fc receptor mediated pathway. To understand these unique functions, it was important to identify their substrates within the GPCR pathway. Genetic and direct biochemical evidences in this paper provide strong support to the hypothesis that CD148 and CD45 both regulate SFKs by targeting their C-terminal negative regulatory tyrosines. However, our studies here show that these two RPTPs regulate the fMLF chemoattractant GPCR induced pathway in distinct ways, namely through the preferential recognition of Lyn by CD148 versus the broader role of CD45 in activating all SFKs, The distinct functions of Hck and Fgr versus Lyn kinase reflect the somewhat unique ability of Lyn to engage inhibitory signaling pathways through specific phosphorylation of ITIM-containing proteins in the plasma membrane and their by regulate their association with cytoplasmic regulatory molecules such as the cytoplasmic tyrosine phosphatase SHP-1 or the cytoplasmic SH2 domain containing inositol lipid 5-phosphatase SHIP-1. Lyn is the primary kinase responsible for phosphorylating inhibitory receptors such as PIR-B, SIRPα, FcRγIIb or cytoplasmic molecules such as Dok1, which in turn recruit phosphatases such as SHP-1 and SHIP-1 to dampen intracellular pathways (Scapini et al., 2009). While Lyn does function in cooperation with other SFKs to initiate activating intracellular signals, its inhibitory function is dominant. Hence, deficiency of the Lyn kinase tends to result in hyperactive immune cells. In contrast, combinatorial loss of Hck and Fgr tends to lead to loss of function (especially when combined with Lyn deficiency). This differential function of SFKs is reflected here in the fMLF signaling pathway as well as in the neutrophil integrin signaling pathway. Lyn-deficient neutrophils show exaggerated adhesion and activation following adhesion to integrin ligands such as ICAM-1, fibrinogen or fibronectin due to reduced recruitment and activation of SHP-1 (Scapini et al., 2009). In contrast, $Hck^{-/-}Fgr^{-/-}$ neutrophils manifest a strong impairment of adhesion-induced functions, including respiratory burst and degranulation (Lowell et al., 1996; Mocsai et al., 1999). In our studies $Hck^{-/-}Fgr^{-/-}$ neutrophils did not show a major defect in the fMLF-mediated pathway, presumably due to the compensatory positive role that Lyn can also play. However, the fact that inducible phosphorylation of SHP-1 is reduced in $Ptprj^{TM-/TM-}$ neutrophils following fMLF stimulation, while it was basally hyperphosphorylated and was normally down-regulated in CD45-deficient cells, provides further biochemical support for the model in which loss of CD148 predominantly disrupts the negative regulatory function of Lyn.

The opposing roles of CD45 and CD148 through their regulation of SFKs on fMLF mediated signaling are intriguing, although it is possible that there are additional substrates for these RPTPs. For example, CD148 may have additional target other than SFK that function only in the inhibitory pathway to modulate the early events in neutrophil GPCR signaling or may influence other pathways altogether. Moreover, the great disparity in the structures of these RPTPs suggests that they may be subject to different modes of regulation yet to be revealed.

EXPERIMENTAL PROCEDURES

Mice

Generation and maintenance of $Ptprc^{-/-}$ mice, $Ptprj^{TM-/TM-}$ mice, and $Ptprc^{-/-}Ptpri^{TM-/TM-}$ mice were described before (Zhu et al., 2008). All animals used in the experiments were at 8–12 weeks of age. All animals were housed in a specific pathogen-free facility at UCSF and were treated according to protocols that were approved by university animal care ethics and veterinary committees and are in accordance with NIH guidelines.

Antibodies and Reagents

Antibodies to murine Gr1, Mac1, Ly6G (1A8) conjugated to PE, PerCP, APC, were from BD Biosciences. Anti-phosphotyrosine antibody 4G10 was from Upstate Biotechnology. Antibodies to phospho-Erk (Thr202 and Tyr204), phospho-Akt (Ser473) and phospho-Lyn (Tyr507) were purchased from Cell Signaling Technology. SH-PTP1 (Santa Cruz C-19), Hck (Santa Cruz M-28) were from Santa Cruz. Lyn antiserum was gift from C. Lowell Lab. Rabbit antiserum to the Src Family Negative Regulatory pY site was from Invitrogen.

Isolation of bone marrow neutrophils

Bone marrow cells were suspended in Ca^{2+} and Mg^{2+}-free HBSS and were layered on the top of 62% Percoll. After centrifugation, neutrophils were harvested from the bottom layer of the Percoll gradient. The purity of the neutrophils, which were detected as $Gr1^+$, $Ly6G^+$, was more than 80%.

In vivo skin abscess infection model

A total of 2×10^7 early exponential phase *S. aureus* (ATCC stain SA113) were injected into a 7-day air pouch created by subcutaneous injection of 5 ml of sterile air on day 1 and reinflation with 3 ml on day 4. After 24 hours (or other indicated time points), the air pouch was lavaged with 3 ml of 0.315% sodium citrate in HBSS. Lavaged cells were enumerated, stained with Ly6G and CD11b for flow cytometry, and an aliquot was lysed in LB with 0.1% Triton X-100. Dilutions were plated on LB agar for viable colony counts. For in vivo chemotaxis assays, *S. aureus* organisms were heat-inactivated at 80°C for 20 minutes before injection.

Neutrophil functional assays

Induction of neutrophil adhesion, oxidative burst, phagocytosis and bactericidal assays were preformed as described before (Lowell et al., 1996; Van Ziffle and Lowell, 2009).

EZ-TAXIScan chamber assay

Bone marrow neutrophils were purified as described before. The EZ-Taxiscan chamber (Effector Cell Institute, Tokyo, Japan) was assembled as per manufacturer instructions. Neutrophils and fMLF in RPMI1640 containing 2% BSA and 20mM HEPES were loaded in opposing chambers and cell migration (at 37°C) was recorded every 30s for 40 min. 260 μm terrace length chips were used with #1.5 Gold Seal cover glasses. The migration movies were analyzed by two independent methods: Cell Tracker software (developed in-house by Angi Chau) and Volocity software (Perkin Elmer). Results presented in this paper were output by Volocity and plotted in statistical graphing software (GraphPad Prism). Only cells that were correctly tracked for at least 50 timepoints (25 minutes) were included in the analysis. Prior to analysis by Volocity software, ImageJ software was used to Subtract Background and to Enhance Local Contrast (CLAHE). MATLAB was also used for figure generation. Movies with cell tracking are available in the supplementary material.

We studied the following migration metrics of interest: track velocity (defined as the total path length between the start and end points of a cell's track divided by the time elapsed; equivalent to the average instantaneous velocity of a cell along its entire track), displacement rate (defined as the straight-line distance between the start and end points of a cell's track divided by the time elapsed), directionality (defined as the straight-line distance between the start and end point of a cell's track (displacement) divided by the total path length.

Flow Cytometry

Single-cell suspensions were prepared from bone marrow (BM) cells. Fc receptors were blocked with rat anti-CD16/CD32 (2.4G2). 10^6 cells were stained with the indicated antibodies. Intracellular Phospho-ERK and Akt staining of BM cells was performed after cells were stimulated with medium or fMLP for indicated time intervals and fixed with 2% paraformaldehyde. Cells were permeabilized with 90% ice-cold methanol, stained with phospho-ERK or phospho-Akt (Cell Signaling Technology), Gr1, and Ly6G antibody and then analyzed on a FACS Calibur (BD).

Calcium Flux

Purified neutrophils were loaded with Fluo-3 AM (1 μg/ml) for 30 min at 37°C in complete culture media. Cells were analyzed by flow cytometry (FACS Calibur) at 37°C and activated by different doses of fMLP. The concentration of intracellular free calcium was measured by Fluo-3 fluorescence.

Protein immunoprecipitation

15×10^6 purified BM neutrophils (for SH-PTP-1) or 40×10^6 BM cells (for Lyn and Hck) were used for each immunoprecipitation. Cells were rested or stimulated and lysed in 1% NP-40 lysis buffer, then subjected to immunoprecipitation with 3μg antibody, which was coupled to protein G agarose beads. SH-PTP1 (Santa Cruz C-19), Hck (Santa Cruz M-28) and Lyn (from C. Lowell Lab) were used for immunoprecipitation (IP). Phosphotyrosine 4G10, anti-SH-PTP1, phospho-Lyn 507 (cell signaling #2731) and Src Family Negative Regulatory pY site (Invitrogen 44–912) antibodies were used for western blots.

Supplementary Material

Refer to Web version on PubMed Central for supplementary material.

Acknowledgments

References

Bjorge JD, Jakymiw A, Fujita DJ. Selected glimpses into the activation and function of Src kinase. Oncogene. 2000; 19:5620–5635. [PubMed: 11114743]

Byth KF, Conroy LA, Howlett S, Smith AJ, May J, Alexander DR, Holmes N. CD45-null transgenic mice reveal a positive regulatory role for CD45 in early thymocyte development, in the selection of CD4+CD8+ thymocytes, and B cell maturation. J Exp Med. 1996; 183:1707–1718. [PubMed: 8666928]

Chan VW, Meng F, Soriano P, DeFranco AL, Lowell CA. Characterization of the B lymphocyte populations in Lyn-deficient mice and the role of Lyn in signal initiation and down-regulation. Immunity. 1997; 7:69–81. [PubMed: 9252121]

DeFranco AL, Chan VW, Lowell CA. Positive and negative roles of the tyrosine kinase Lyn in B cell function. Semin Immunol. 1998; 10:299–307. [PubMed: 9695186]

Ellson CD, Davidson K, Ferguson GJ, O'Connor R, Stephens LR, Hawkins PT. Neutrophils from p40phox−/− mice exhibit severe defects in NADPH oxidase regulation and oxidant-dependent bacterial killing. J Exp Med. 2006; 203:1927–1937. [PubMed: 16880254]

Fitzer-Attas CJ, Lowry M, Crowley MT, Finn AJ, Meng F, DeFranco AL, Lowell CA. Fcgamma receptor-mediated phagocytosis in macrophages lacking the Src family tyrosine kinases Hck, Fgr, and Lyn. J Exp Med. 2000; 191:669–682. [PubMed: 10684859]

Foxman EF, Campbell JJ, Butcher EC. Multistep navigation and the combinatorial control of leukocyte chemotaxis. J Cell Biol. 1997; 139:1349–1360. [PubMed: 9382879]

Fumagalli L, Zhang H, Baruzzi A, Lowell CA, Berton G. The Src family kinases Hck and Fgr regulate neutrophil responses to N-formyl-methionyl-leucyl-phenylalanine. J Immunol. 2007; 178:3874–3885. [PubMed: 17339487]

Gaya A, Pirotto F, Palou E, Autschbach F, Del Pozo V, Sole J, Serra-Pages C. CD148, a new membrane tyrosine phosphatase involved in leukocyte function. Leuk Lymphoma. 1999; 35:237–243. [PubMed: 10706446]

Heit B, Tavener S, Raharjo E, Kubes P. An intracellular signaling hierarchy determines direction of migration in opposing chemotactic gradients. J Cell Biol. 2002; 159:91–102. [PubMed: 12370241]

Hermiston ML, Xu Z, Majeti R, Weiss A. Reciprocal regulation of lymphocyte activation by tyrosine kinases and phosphatases. J Clin Invest. 2002; 109:9–14. [PubMed: 11781344]

Hermiston ML, Xu Z, Weiss A. CD45: a critical regulator of signaling thresholds in immune cells. Annu Rev Immunol. 2003; 21:107–137. [PubMed: 12414720]

Hermiston ML, Zikherman J, Zhu JW. CD45, CD148, and Lyp/Pep: critical phosphatases regulating Src family kinase signaling networks in immune cells. Immunological reviews. 2009; 228:288–311. [PubMed: 19290935]

Hibbs ML, Harder KW, Armes J, Kountouri N, Quilici C, Casagranda F, Dunn AR, Tarlinton DM. Sustained activation of Lyn tyrosine kinase in vivo leads to autoimmunity. J Exp Med. 2002; 196:1593–1604. [PubMed: 12486102]

Hibbs ML, Tarlinton DM, Armes J, Grail D, Hodgson G, Maglitto R, Stacker SA, Dunn AR. Multiple defects in the immune system of Lyn-deficient mice, culminating in autoimmune disease. Cell. 1995; 83:301–311. [PubMed: 7585947]

Jakus Z, Fodor S, Abram CL, Lowell CA, Mocsai A. Immunoreceptor-like signaling by beta 2 and beta 3 integrins. Trends in cell biology. 2007; 17:493–501. [PubMed: 17913496]

Kim MH, Liu W, Borjesson DL, Curry FR, Miller LS, Cheung AL, Liu FT, Isseroff RR, Simon SI. Dynamics of neutrophil infiltration during cutaneous wound healing and infection using fluorescence imaging. The Journal of investigative dermatology. 2008; 128:1812–1820. [PubMed: 18185533]

Kishihara K, Penninger J, Wallace VA, Kundig TM, Kawai K, Wakeham A, Timms E, Pfeffer K, Ohashi PS, Thomas ML, et al. Normal B lymphocyte development but impaired T cell maturation in CD45-exon6 protein tyrosine phosphatase-deficient mice. Cell. 1993; 74:143–156. [PubMed: 8334701]

Li Y, Karlin A, Loike JD, Silverstein SC. A critical concentration of neutrophils is required for effective bacterial killing in suspension. Proceedings of the National Academy of Sciences of the United States of America. 2002; 99:8289–8294. [PubMed: 12060772]

Liese J, Kloos S, Jendrossek V, Petropoulou T, Wintergerst U, Notheis G, Gahr M, Belohradsky BH. Long-term follow-up and outcome of 39 patients with chronic granulomatous disease. J Pediatr. 2000; 137:687–693. [PubMed: 11060536]

Lin J, Zhu JW, Baker JE, Weiss A. Regulated expression of the receptor-like tyrosine phosphatase CD148 on hemopoietic cells. J Immunol. 2004; 173:2324–2330. [PubMed: 15294945]

Liu L, Puri KD, Penninger JM, Kubes P. Leukocyte PI3Kgamma and PI3Kdelta have temporally distinct roles for leukocyte recruitment in vivo. Blood. 2007; 110:1191–1198. [PubMed: 17488877]

Lowell CA. Src-family kinases: rheostats of immune cell signaling. Mol Immunol. 2004; 41:631–643. [PubMed: 15220000]

Lowell CA, Fumagalli L, Berton G. Deficiency of Src family kinases p59/61hck and p58c-fgr results in defective adhesion-dependent neutrophil functions. J Cell Biol. 1996; 133:895–910. [PubMed: 8666673]

Luttrell LM, Daaka Y, Lefkowitz RJ. Regulation of tyrosine kinase cascades by G-protein-coupled receptors. Curr Opin Cell Biol. 1999; 11:177–183. [PubMed: 10209148]

Mee PJ, Turner M, Basson MA, Costello PS, Zamoyska R, Tybulewicz VL. Greatly reduced efficiency of both positive and negative selection of thymocytes in CD45 tyrosine phosphatase-deficient mice. Eur J Immunol. 1999; 29:2923–2933. [PubMed: 10508267]

Mocsai A, Jakus Z, Vantus T, Berton G, Lowell CA, Ligeti E. Kinase pathways in chemoattractant-induced degranulation of neutrophils: the role of p38 mitogen-activated protein kinase activated by Src family kinases. J Immunol. 2000; 164:4321–4331. [PubMed: 10754332]

Mocsai A, Ligeti E, Lowell CA, Berton G. Adhesion-dependent degranulation of neutrophils requires the Src family kinases Fgr and Hck. J Immunol. 1999; 162:1120–1126. [PubMed: 9916742]

Murphy PM. The molecular biology of leukocyte chemoattractant receptors. Annu Rev Immunol. 1994; 12:593–633. [PubMed: 8011292]

Nishizumi H, Taniuchi I, Yamanashi Y, Kitamura D, Ilic D, Mori S, Watanabe T, Yamamoto T. Impaired proliferation of peripheral B cells and indication of autoimmune disease in lyn-deficient mice. Immunity. 1995; 3:549–560. [PubMed: 7584145]

Pollock JD, Williams DA, Gifford MA, Li LL, Du X, Fisherman J, Orkin SH, Doerschuk CM, Dinauer MC. Mouse model of X-linked chronic granulomatous disease, an inherited defect in phagocyte superoxide production. Nat Genet. 1995; 9:202–209. [PubMed: 7719350]

Sasaki AT, Firtel RA. Regulation of chemotaxis by the orchestrated activation of Ras, PI3K, and TOR. Eur J Cell Biol. 2006; 85:873–895. [PubMed: 16740339]

Sasaki T, Irie-Sasaki J, Jones RG, Oliveira-dos-Santos AJ, Stanford WL, Bolon B, Wakeham A, Itie A, Bouchard D, Kozieradzki I, et al. Function of PI3Kgamma in thymocyte development, T cell activation, and neutrophil migration. Science. 2000; 287:1040–1046. [PubMed: 10669416]

Scapini P, Pereira S, Zhang H, Lowell CA. Multiple roles of Lyn kinase in myeloid cell signaling and function. Immunological reviews. 2009; 228:23–40. [PubMed: 19290919]

Sicheri F, Kuriyan J. Structures of Src-family tyrosine kinases. Curr Opin Struct Biol. 1997; 7:777–785. [PubMed: 9434895]

Stephens L, Ellson C, Hawkins P. Roles of PI3Ks in leukocyte chemotaxis and phagocytosis. Curr Opin Cell Biol. 2002; 14:203–213. [PubMed: 11891120]

Stephens L, Smrcka A, Cooke FT, Jackson TR, Sternweis PC, Hawkins PT. A novel phosphoinositide 3 kinase activity in myeloid-derived cells is activated by G protein beta gamma subunits. Cell. 1994; 77:83–93. [PubMed: 8156600]

Stoyanov B, Volinia S, Hanck T, Rubio I, Loubtchenkov M, Malek D, Stoyanova S, Vanhaesebroeck B, Dhand R, Nurnberg B, et al. Cloning and characterization of a G protein-activated human phosphoinositide-3 kinase. Science. 1995; 269:690–693. [PubMed: 7624799]

Van Ziffle JA, Lowell CA. Neutrophil-specific deletion of Syk kinase results in reduced host defense to bacterial infection. Blood. 2009; 114:4871–4882. [PubMed: 19797524]

Viola A, Luster AD. Chemokines and their receptors: drug targets in immunity and inflammation. Annu Rev Pharmacol Toxicol. 2008; 48:171–197. [PubMed: 17883327]

Wu D, LaRosa GJ, Simon MI. G protein-coupled signal transduction pathways for interleukin-8. Science. 1993; 261:101–103. [PubMed: 8316840]

Yu CC, Yen TS, Lowell CA, DeFranco AL. Lupus-like kidney disease in mice deficient in the Src family tyrosine kinases Lyn and Fyn. Curr Biol. 2001; 11:34–38. [PubMed: 11166177]

Zhang H, Meng F, Chu CL, Takai T, Lowell CA. The Src family kinases Hck and Fgr negatively regulate neutrophil and dendritic cell chemokine signaling via PIR-B. Immunity. 2005; 22:235–246. [PubMed: 15723811]

Zhang Z, Shen K, Lu W, Cole PA. The role of C-terminal tyrosine phosphorylation in the regulation of SHP-1 explored via expressed protein ligation. J Biol Chem. 2003; 278:4668–4674. [PubMed: 12468540]

Zhu JW, Brdicka T, Katsumoto TR, Lin J, Weiss A. Structurally distinct phosphatases CD45 and CD148 both regulate B cell and macrophage immunoreceptor signaling. Immunity. 2008; 28:183–196. [PubMed: 18249142]
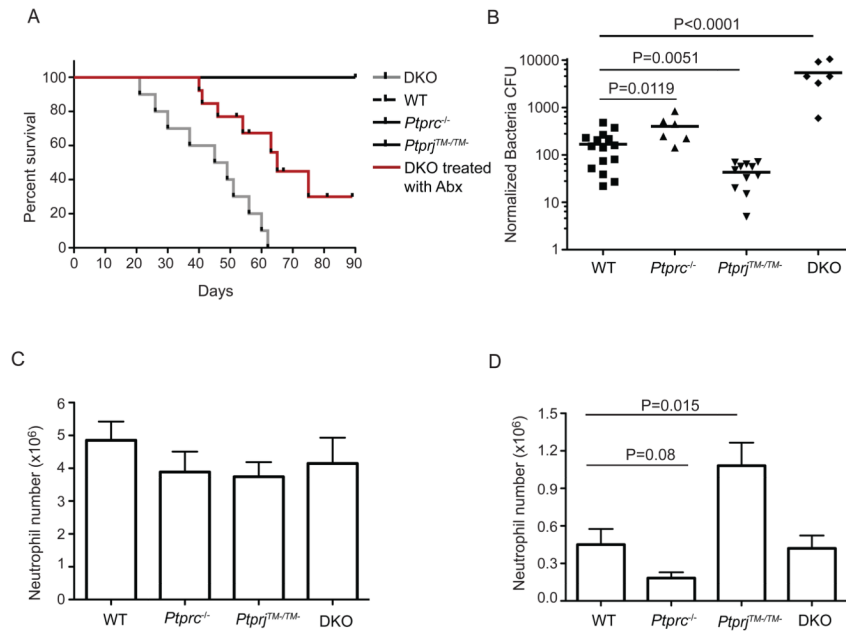
Figure 1. Distinct functions of CD45 and CD148 in bacterial clearance

(**A**) Mortality curves of mice of the indicated genotypes are shown, where n = 10 for each genotype. DKO refers to $Ptprc^{-/-} Ptprj^{TM-/TM-}$ double mutant mice. DKO** were DKO mice treated with food tablets containing amoxicillin (3 mg), Flagyl (0.69 mg) and bismouth (1.185 mg) (1 tablet/cage/week). The difference between DKO and DKO** group is statistically significant (p<0.0001). (**B**) Animals of indicated genotypes were infected with S. *aureus* in the air pouch. After 24hr infection, live bacteria in the air pouch were collected by lavage. Recovered Colony Forming Units (CFU) of *S. aureus* from each mouse were counted and shown. Each symbol represents an individual mouse. Small horizontal lines indicate the means. Bacterial CFU was normalized between experiments based on their bacterial input. CFU shown is following an initial 10^2 dilution. (**C**) Neutrophil accumulation in the air pouch after 24 hr of *S. aureus* infection. Neutrophil counts were determined as (cell count from infected air pouch) $\times$ (percentage of neutrophils, identified as CD11b$^+$ and Gr1$^+$ by flow cytometry). (**D**) Neutrophil recruitment 6 hr after injection of heat inactivated *S. aureus*. (**C,D**) Data are presented as mean $\pm$ SEM; p values were calculated by the student t test. For (**B**) and (**C**), n=16 wild type mice, n=5 $Ptprc^{-/-}$ mice, n=12 $Ptprj^{TM-/TM-}$ mice, n=5 DKO mice were used for experiments. For (**D**), n=9 wild type mice, n=8 $Ptprc^{-/-}$ mice, n=9 $Ptprj^{TM-/TM-}$ mice, n=6 DKO mice were used for experiments.
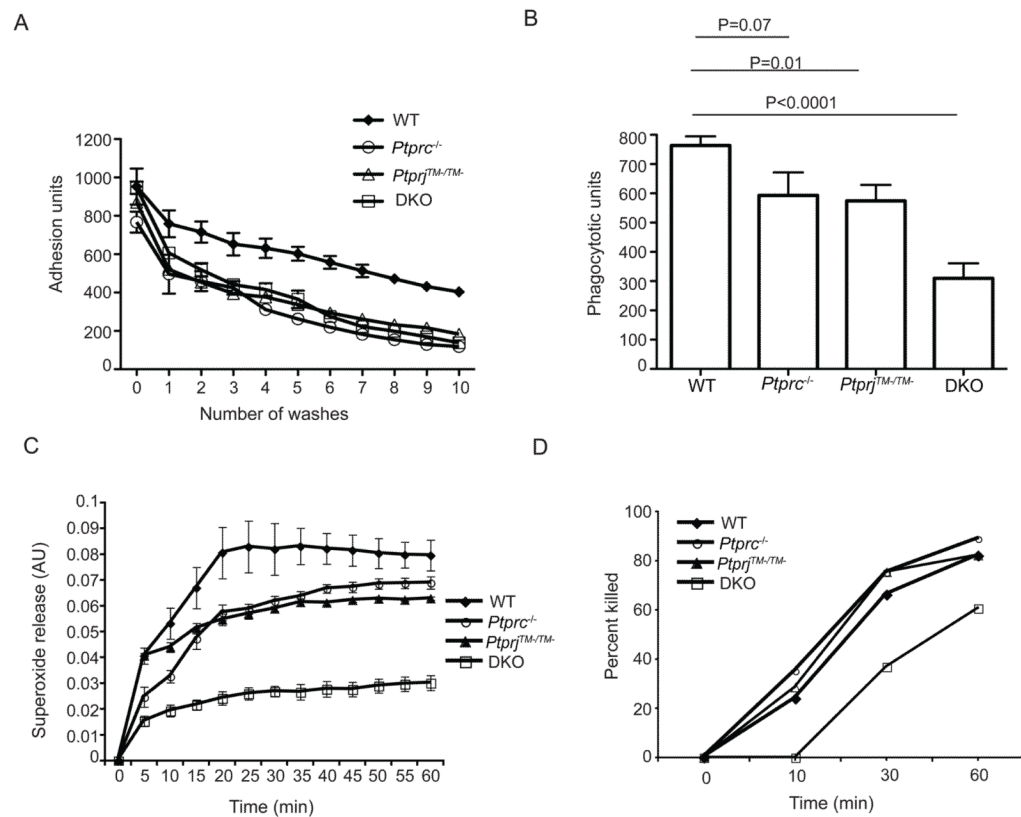
A

B

C

D

Figure 2. CD45 and CD148 redundantly regulate neutrophil adhesion, phagocytosis, superoxide production and bacterial killing

(**A**) Fluorescently labeled BM PMNs from indicated mice were plated on pRGD-coated wells and allowed to adhere at 37°C for 15 min, then exposed to a series of washes in a static adhesion assay. The decrease in fluorescence corresponding to the decrease in cell number was measured and plotted over the series of washes. Error bars represent ± SEM of triplicate samples. (**B**) Phagocytosis was determined by flow cytometric analysis of FITC-labeled heat inactivated opsonized *S. aureus* that were phagocytosed by neutrophils purified from mice of the indicated genotypes. Phagocytic units were calculated as (MFI of FITC+ neutrophils) X (% of FITC+ neutrophils). The data points shown here were determined 15 min. after bacteria incubation. Data were pooled from six independent experiments. The graph shows mean ± SEM. (**C**) Purified neutrophils were plated on microtiter wells in cytochrome c containing media. Production of superoxide by a respiratory burst following 1μm fMLF treatment was measured as the reduction of cytochrome c. Data were pooled from three independent experiments. (**D**) Intracellular bacterial killing capacity was assessed by viable S. *aureus* colony forming units (CFU). Percentage of killing was calculated as (1-(remaining CFU/input CFU)) X 100. Data were pooled from three independent experiments.
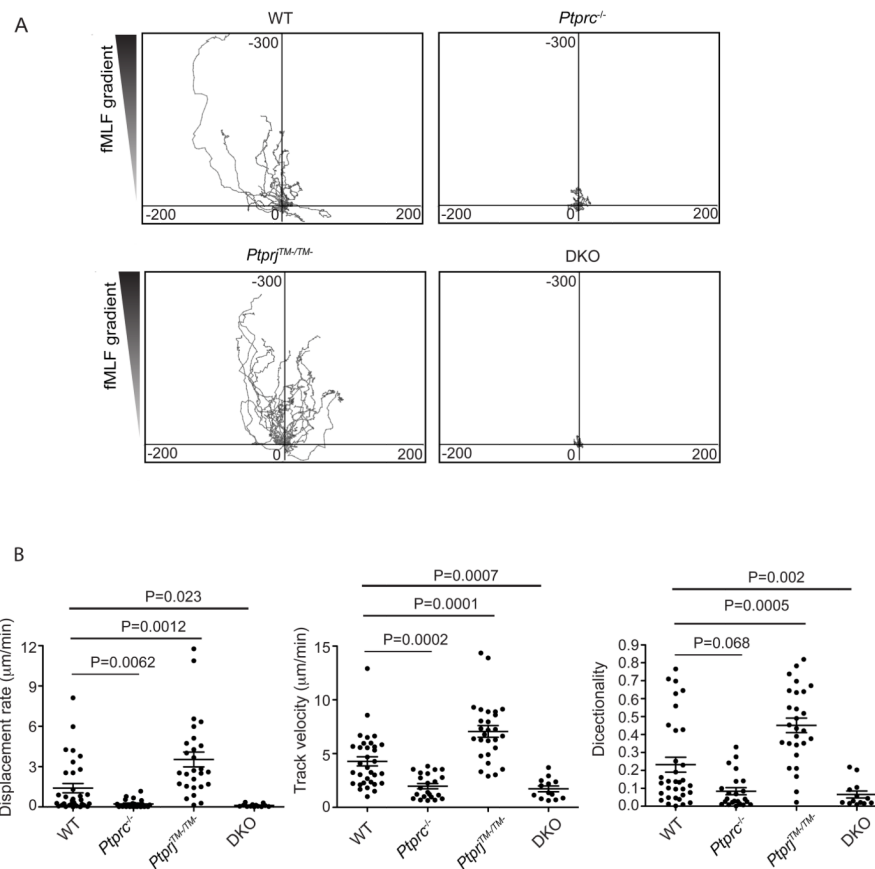
Figure 3. CD45 and CD148 regulate neutrophil chemotaxis in a distinct ways
(**A**) Center-zeroed tracks of individual neutrophils in an EZ-Taxiscan chamber migrating towards reservoirs, located at the top of the diagrams, containing 3 μM fMLF. The scales of each graph are equal in μm. (**B**) Statistical analysis for the EZ-Taxiscan migration assay. Displacement rate (μm min^{-1}), track velocity (μm min^{-1}) and directionality (ratio of displacement to track, value 1 as maximum) were calculated by Volocity^{TM}. Each symbol represents an individual cell; small horizontal lines indicate means. p values were calculated by the student t test. See also Fig. S1, Movie M1,M2,M3,M4.
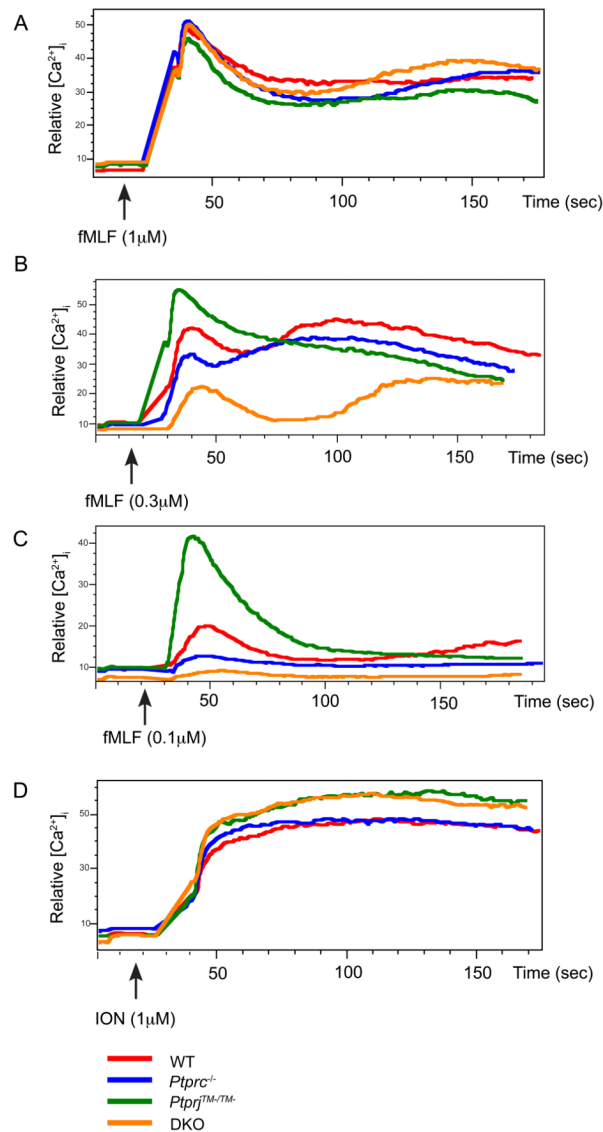
Figure 4. CD45 and CD148 differentially regulate fMLP mediated increase of intracellular Ca^{2+} in dose dependent manner

Purified neutrophils from mice of the indicated genotypes were loaded with Fluo3-AM and Fura Red, then intracellular free-Ca^{2+} concentrations were monitored before and after addition of different dose of fMLF **(A), (B), (C)** or ionomycin **(D).** Data are representative of three independent experiments.
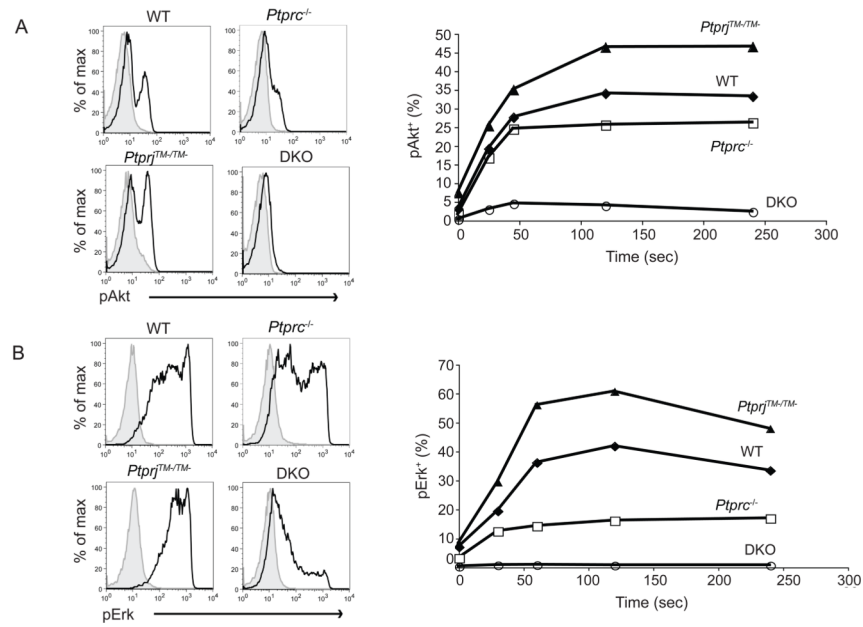
Figure 5. CD45 and CD148 differentially regulate signaling events following fMLF stimulation
(A) BM cells from mice of the indicated genotypes were stimulated with fMLF (0.2 μM) for indicated time, fixed, permeabilized, and then stained with phospho-Akt along with other surface makers. Neutrophils were identified as CD11b$^+$Gr1$^+$. Phospho-Akt of stimulated (2.5 min, shown as black lines) and control samples (shown as filled histograms) were overlaid. Percentages of pAkt$^+$ cells over a time course are shown on the right side. Data are representative of three independent experiments. **(B)** BM cells were treated same as in **(A)** and phospho-ERK was stained similarly. Percentages of pERK$^+$ cells over a time course are shown on the right side. Data are representative of three independent experiments.
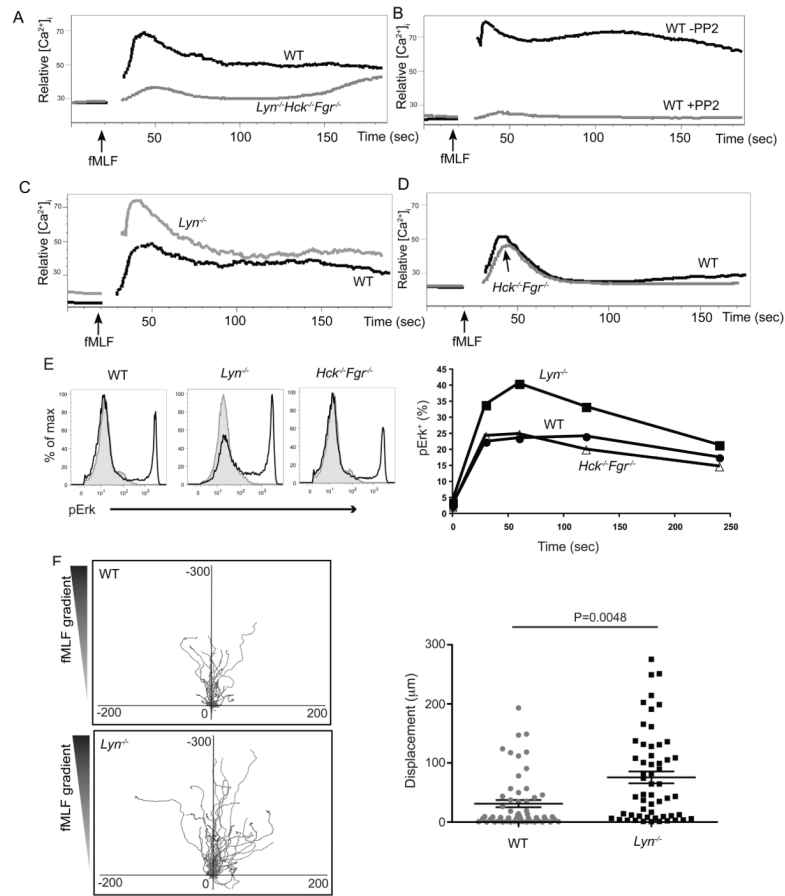
Figure 6. Disruption of SFKs results in impairment on fMLF induced signaling
(A) Purified neutrophils from mice of the indicated genotypes were loaded with Fluo3-AM and Fura Red, and $[Ca^{2+}]_i$ concentrations were monitored before and after addition of 0.2 μm fMLF. **(B)** Wild-type neutrophils were treated similarly as in **(A)**, however prior to addition of fMLF, cells were incubated with or without 10 μm PP2 for 3 minutes. **(C) (D)** Neutrophils from wild-type, $Lyn^{-/-}$ **(C),** or wild-type, $Hck^{-/-}Fgr^{-/-}$ **(D)** mice were treated similarly as in **(A)**. **(E)** BM cells from mice of the indicated genotypes were stimulated with fMLF (0.5 μM) for the indicated times, fixed, permeabilized, and then stained with phospho-ERK along with other surface makers. Neutrophils were identified as CD11b+Gr1+. Phospho-ERK of stimulated (1 min) and control samples were overlaid as histograms (control as grey shade and stimulated as black line). Percentages of pERK+ cells over a time course are shown on the right side. Data are representative of three independent experiments. **(F)** fMLF mediated chemotaxis was measured on an EZ-Taxiscan chamber as shown in Fig. 3. Left panel shows center-zeroed tracks of individual neutrophils on migrating towards reservoirs, located at the top of the diagrams, containing 0.5 μM fMLF. The scale of each graph is equal in μm. Right panel is a statistical analysis for the EZ-Taxiscan migration assay. p values were calculated by student t test. See also Fig. S3, Movie M5, M6.
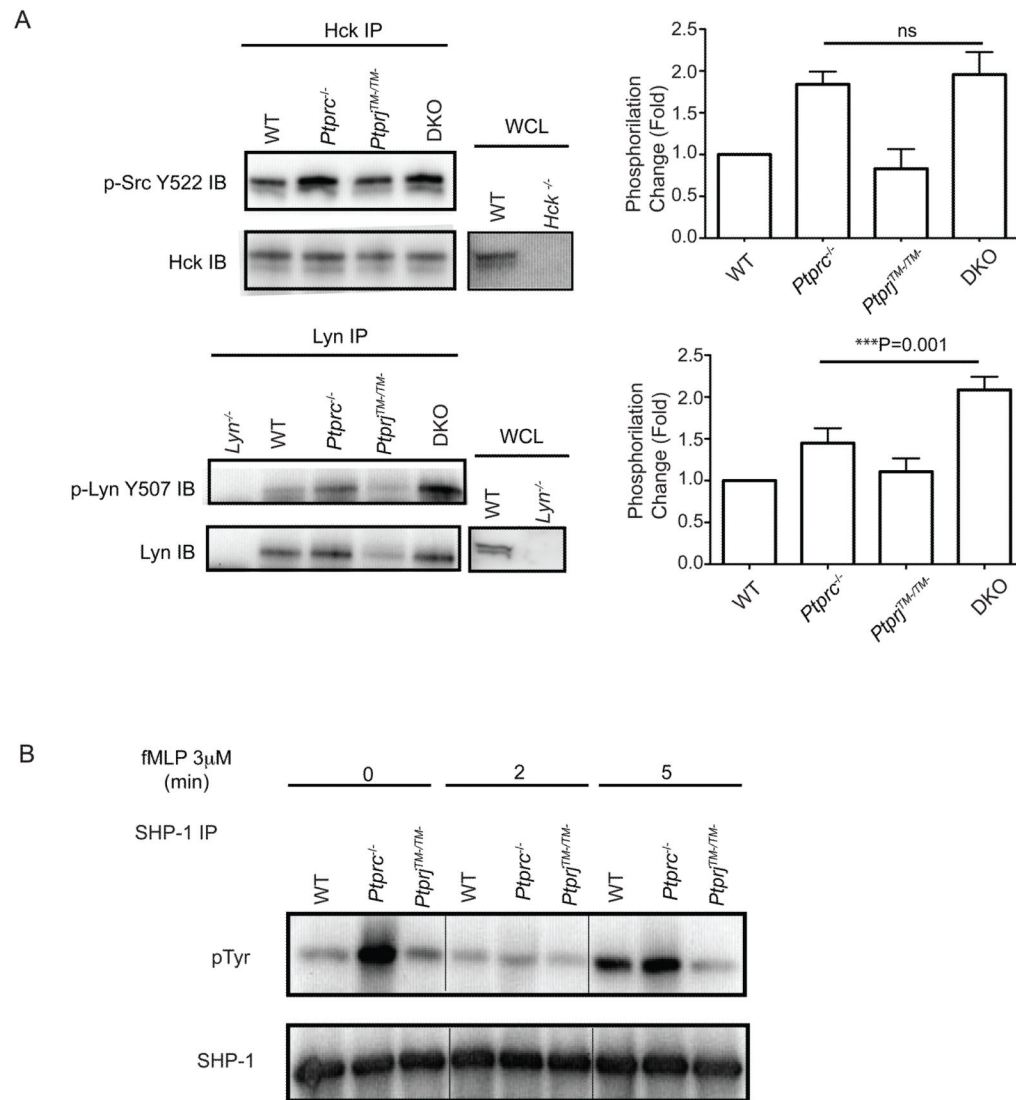
Figure 7.
(A) BM cells (40×10^6/sample) were harvested and then lysed. Hck or Lyn was immunoprecipitated and subject to immunoblotting with antiphosphotyrosine (pTyr) Abs or anti-Hck and Lyn for loading controls. Specificities of Hck and Lyn Abs were confirmed with whole cell lysates from $Hck^{-/-}$ or $Lyn^{-/-}$ mice. Quantification of inhibitory tyrosine phosphorylation amounts were normalized to loading controls and the fold changes relative to wild type were graphed. For Hck n=3 and for Lyn n=4. **(B)** Neutrophils (15×10^6/sample) were treated with fMLP (3μm) for indicated times and then lysed. SHP-1 was immunoprecipitated and subjected to immunoblotting with antiphosphotyrosine (pTyr) Ab 4G10 or SHP-1 as a loading control. Data are representative of three independent experiments. See also Fig. S4.